Proceedings of the 1998 IEEE
International Conference on Robotics & Automation
Leuven, Belgium • May 1998

Biped Robot Walking Using Gravity-Compensated Inverted Pendulum Mode and Computed Torque Control

Jong H. Park and Kyoung D. Kim

Mechatronics Lab
School of Mechanical Engineering
Hanyang University
Seoul, 133-791, Korea
Email: jongpark@email.hanyang.ac.kr

Abstract

This paper proposes a model called the gravity-compensated inverted pendulum mode (GCIPM) to generate a biped locomotion pattern that is similar to the one generated by the linear inverted pendulum mode, but accommodates the free leg dynamics based upon its predetermined trajectory. When the biped locomotion based upon the linear inverted pendulum mode is applied to real biped robots, the stability of the robot is disturbed due to the fact that the neglected dynamics of free legs is not actually negligible, moving the ZMP (zero moment point) away from the presumed fixed point. The GCIPM includes the effect of the dynamics of the free leg in a simple manner. This paper also presents a control method for biped robots based upon the computed torque. Simulation results show that the biped robot is more stable with the walking pattern generated by the proposed method combined with the controller than with the one by the inverted pendulum mode.

1 Introduction

In the area of biped robot walking control, one of the most important research areas is the design of reference motions of biped robots. One of the methods to generate dynamic walking pattern for biped robots was proposed [1, 2] based upon so-called the ZMP-equation. However, since this method solves all the dynamic equations with some assumptions, it is complicated and thus demanding a substantial computing power of the controller to implement. A simpler method called the linear inverted pendulum mode was also proposed by Kajita and Tani [3, 4]. This method is usually used to generate reference motions since they are very similar to the human biped locomotion. It generates the reference motion of the base link under the assumption that all the masses of the entire biped robot system are concentrated at the CG (center of gravity) point of the base link and that the ground exerts a pushing force but not a moment at the center of the foot in contact with it. From the reference motion trajectory of the base, the trajectories of all the joints of the supporting leg can be generated.

However, when the trajectory generated by the inverted pendulum mode is applied to a real biped robot whose legs have nonzero masses and moments of inertia, the ZMP (zero moment point) moves away from the presumed fixed point and the stability of the biped robot is badly compromised by the neglected dynamics of free leg motions [5]. Therefore, we propose a new method called the gravity-compensated inverted pendulum mode (GCIPM) to design reference motions of biped robots based on the linear inverted pendulum mode, but including the effect the free leg motion dynamics. This method assumes that the biped robot consists of two different masses instead of a single mass as in the inverted pendulum mode. One mass is for both the base link and the supporting leg, and the other is for the free leg. By separating the two masses, more "precise" locomotion can be generated. Since this method assumes that the gravity of the free leg is the most dominant in its dynamic equation, a simple trajectory of the base link in a closed form is obtained as in the case of the inverted pendulum mode.

In Section 2, the dynamic model of the biped robot is formulated. Section 3 describes the GCIPM and its application to the design of the reference motion of the biped robot. Section 4 explains the servo controller design method based upon the computed torque control method. In Section 5, the computer simulations of a 7-link biped robot to compare the performance of the proposed GCIPM and the linear inverted pendulum mode are explained with their results. We finally summarize conclusions in Section 6.

0-7803-4300-x-5/98 $10.00 © 1998 IEEE

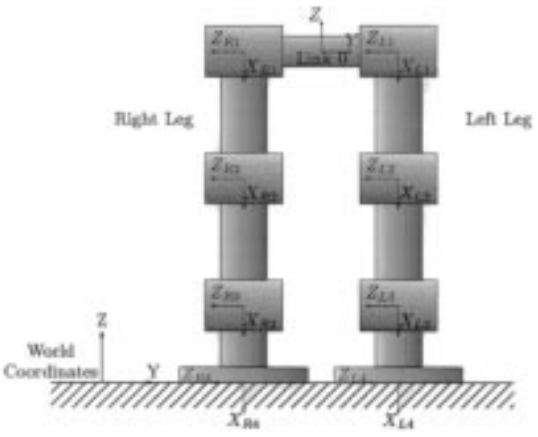

Figure 1: A 7-link biped robot and its coordinates.

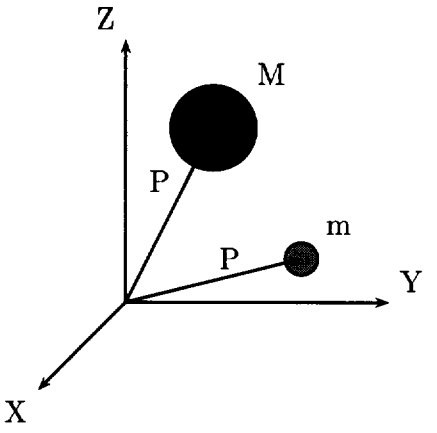

Figure 2: The simple biped robot model to generate a locomotion by GCIPM consists of 2 masses.

2 The Model of Biped Robot

Biped robots have a structure of multiple closed-chain mechanism. Figure 1 shows the 7-link biped robot used in this paper. The base coordinate frame is attached to the moving base link, link 0, of the robot [6] rather than fixed to the ground as the Newtonian frame. The Denavit-Hartenberg notation is used to describe the kinematics of the biped robot.

The direct dynamic model of the multiple closed chain mechanism [6] can be simply extended from a single open chain mechanism [7]. First, the dynamic equation for the left and right legs is

$$\begin{bmatrix}\boldsymbol{\tau}_\ell \\ \boldsymbol{\tau}_r\end{bmatrix} = \begin{bmatrix}\mathbf{H}_\ell & \mathbf{0} \\ \mathbf{0} & \mathbf{H}_r\end{bmatrix}\begin{bmatrix}\ddot{\mathbf{q}}_\ell \\ \ddot{\mathbf{q}}_r\end{bmatrix} + \begin{bmatrix}\mathbf{K}_\ell \\ \mathbf{K}_r\end{bmatrix}\mathbf{a}_0 + \begin{bmatrix}\mathbf{N}_\ell \\ \mathbf{N}_r\end{bmatrix} + \begin{bmatrix}\mathbf{D}_\ell & \mathbf{0} \\ \mathbf{0} & \mathbf{D}_r\end{bmatrix}\begin{bmatrix}\mathbf{f}_\ell \\ \mathbf{f}_r\end{bmatrix} \quad (1)$$

where $\boldsymbol{\tau}_\ell, \boldsymbol{\tau}_r \in \mathbb{R}^3$ are the joint torque vectors for the legs, $\mathbf{q}_\ell, \mathbf{q}_r \in \mathbb{R}^3$ are the joint angle vectors, $\mathbf{H}_\ell, \mathbf{H}_r \in \mathbb{R}^3$ are the inertia matrices, $\mathbf{a}_0 \in \mathbb{R}^6$ is the acceleration of the base link, $\mathbf{N}_\ell, \mathbf{N}_r \in \mathbb{R}^3$ are the terms related to the Coriolis and centripetal accelerations, and the gravity for the links, and $\mathbf{f}_\ell, \mathbf{f}_r \in \mathbb{R}^3$ are the external reaction force and moment vectors from the ground to the feet of the robot. Subscript 'ℓ' and 'r' denote the left and right leg links and subscript '0' represents the base link (link 0).

The couplings among the motions of the left and the right leg, and the motion of the base link can be expressed by

$$\mathbf{0} = \begin{bmatrix}\mathbf{Q}_\ell & \mathbf{Q}_r\end{bmatrix}\begin{bmatrix}\ddot{\mathbf{q}}_\ell \\ \ddot{\mathbf{q}}_r\end{bmatrix} + \mathbf{R}\mathbf{a}_0 + \mathbf{S} + \begin{bmatrix}\mathbf{P}_\ell & \mathbf{P}_r\end{bmatrix}\begin{bmatrix}\mathbf{f}_\ell \\ \mathbf{f}_r\end{bmatrix}. \quad (2)$$

The kinematic constraint that the foot of the supporting leg is in contact with the ground is expressed by

$$\mathbf{0} = \mathbf{A}_s\ddot{\mathbf{q}}_s + \mathbf{B}_s\mathbf{a}_0 + \mathbf{C}_s. \quad (3)$$

All the parameters used in Eq. (1), (2) and (3) can be computed analytically or numerically. In this paper, they are numerically computed using the Newton-Euler inverse dynamics [8].

3 Reference Motion Design of Biped Robot

3.1 Gravity-Compensated Inverted Pendulum Mode (GCIPM)

The biped locomotion generated by the linear inverted pendulum mode and a fixed ZMP results in large movements of the ZMP. The range of the ZMP movements determines the degree of the stability of the biped robot. Such movements of the ZMP is due to the approximation that all the masses are concentrated at a single point of the base link. However, all the links have a nonzero mass and therefore their dynamics influences the motion of the biped robot. Especially, the disturbance due to the dynamics of the free leg with nonzero mass significantly disturbs the balance in the sagittal plane due to its mass and dynamic motion, and thus moves the ZMP around.

In the GCIPM that we propose in this paper, the biped robot is considered to be divided into two parts: the free leg and the rest of the body. By having a slightly more detailed model of the robot, i.e., two separate parts rather than a single mass as in the inverted pendulum mode, more accurate motion can be applied for higher stability. The GCIPM assumes that the mass of the free leg is concentrated at its foot and that the mass of the rest of the body is concentrated at

the base link as in the inverted pendulum mode. Figure 2 shows a simple biped robot model for the GCIPM, which consists of two parts. In this figure, M is the mass of the biped robot excluding the free leg and m is the mass of the free leg. From this model, we can easily derive the moment equation about the ZMP.

$$\mathbf{P} \times (M\ddot{\mathbf{P}}) = -\mathbf{p} \times (m\ddot{\mathbf{p}}) + \mathbf{P} \times (M\mathbf{g}) + \mathbf{p} \times (m\mathbf{g}) \tag{4}$$

where $\mathbf{P} = [X \quad Y \quad Z]^T$, $\mathbf{p} = [x \quad y \quad z]^T$, and $\mathbf{g} = [0 \quad 0 \quad -g]^T$, representing the gravity vector.

In this paper, only the biped motion in the sagittal plane is considered. Assuming that $Y = y = 0$ and $Z = H_z =$ constant (the height of base link from the ground) and considering the Y-directional components in Eq. (4),

$$\ddot{X} - \omega^2 X = F(t) \tag{5}$$

where $F(t) = \beta(gx + z\ddot{x} - x\ddot{z})$, $\omega = \sqrt{g/H_z}$ and $\beta = m/M/H_z$.

Term $F(t)$ represents the effect of the free leg dynamics on the CG motion. If the trajectory of the free leg is known, its influence to the rest of the body and therefore the inverted pendulum motion of the CG of biped robot can be computed.

Thus, the trajectory of the free leg (more precisely its foot) should be decided first. The GCIPM does not assume a particular set of trajectories for the foot of the free leg. In this paper, a trajectory that is parabolic in the $xz-$plane is used for the foot of the free leg, which is represented by

$$x(t) = -S\cos(\omega_f t) \qquad \text{for} \quad 0 \le t \le T \tag{6}$$

$$z(t) = \frac{h_f}{2}[1 - \cos(2\omega_f t)] \qquad \text{for} \quad 0 \le t \le T \tag{7}$$

where S is the stride, h_f is the maximum foot height, T is the one step period, and the stride frequency $\omega_f = \pi/T$. An example of the foot motion of the free leg with $T = 1$s, $S = 0.2$m and $h_f = 0.1$m is shown in Fig. 3.

In addition, if we select T and h_f such that $h_f\omega_T^2 \ll g$, $F(t)$ in Eq. (5) becomes a simple function

$$F(t) \approx -\beta g S\cos(\omega_f t) \tag{8}$$

which means that the dynamics of the free leg is dominated by its gravity term. Then, the solution of Eq. (5) is

$$X(t) = C_1 e^{\omega t} + C_2 e^{-\omega t} + \eta\cos(\omega_f t) \tag{9}$$

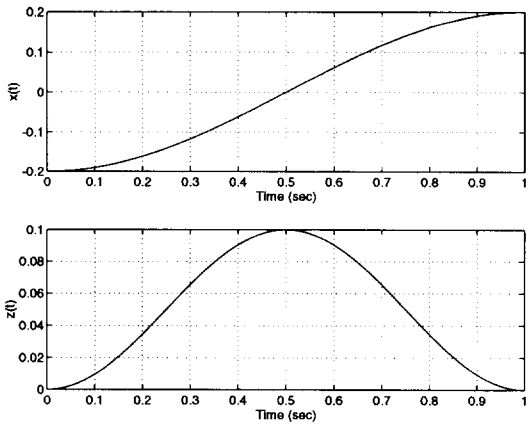

Figure 3: The foot motion of the free leg.

where

$$C_1 = \frac{1}{2}\left(X(0) + \frac{1}{\omega}\dot{X}(0) - \eta\right)$$

$$C_2 = \frac{1}{2}\left(X(0) - \frac{1}{\omega}\dot{X}(0) - \eta\right)$$

$$\eta = \frac{\beta g S}{\omega^2 + \omega_f^2}$$

Variable $X(0)$ and $\dot{X}(0)$ are the initial position and the initial velocity, respectively, of the CG of the biped robot.

Notice that from the above GCIPM solution, the mode is rightly the linear inverted pendulum mode if the free leg mass m is zero.

3.2 Repeatability Conditions

For the biped robot to have steady and repeatable walking pattern, the following repeatability condition should be satisfied.

$$X(0) = -X(T) \quad \text{and} \quad \dot{X}(0) = \dot{X}(T). \tag{10}$$

From this, the initial velocity of the CG can be found.

$$\dot{X}(0) = \frac{1 + e^{\omega T}}{1 - e^{\omega T}}(X(0) - \eta)\,\omega. \tag{11}$$

4 Servo Controller Design

Different servo controllers for the left and the right legs are used based upon the computed torque. For the free (unconstrained) leg, the computed torque controller is used in a similar manner to ones for robot manipulators; and for the supporting (constrained) leg, the controller uses the computed torque so that the error dynamics of the base link position rather than joint angles becomes stable.

Since different controllers are used depending whether a leg is 'free' or 'supporting', subscript 'f' and 's' are used to denote the free and the supporting legs, respectively, in the rest of the paper.

4.1 Free Leg Joint Servo Controller

In the case of a single support phase, the free leg is considered as a robot manipulator. Therefore, the computed torque joint control law [9] is used for the free leg.

Since the free leg is not in contact with the environment, the ground force $\mathbf{f}_f$ is zero. Thus the free leg dynamics in Eq. (1) can be expressed as

$$\tau_f = \mathbf{H}_f \ddot{\mathbf{q}}_f + \mathbf{K}_f \mathbf{a}_0 + \mathbf{N}_f. \tag{12}$$

We can control the free leg to tracking the reference joint trajectory which is obtained from the reference motion of CG, the reference motion of free leg tip and numerical inverse kinematics [10] of that chain. After all, the free leg control input torque is calculated from the following equation.

$$\tau_f = \mathbf{H}_f(\ddot{\mathbf{q}}_f^d - \mathbf{u}_f) + \mathbf{K}_f \mathbf{a}_0 + \mathbf{N}_f \tag{13}$$

where $\ddot{\mathbf{q}}_f^d$ is the reference joint acceleration of the free leg, and $\mathbf{u}_f$ is the linear error feedback control signal. In this paper, a PD controller is used so that

$$\mathbf{u}_f = -\mathbf{K}_v \dot{\mathbf{e}}_f - \mathbf{K}_p \mathbf{e}_f$$

where

$$\mathbf{e}_f = \mathbf{q}_f^d - \mathbf{q}_f$$

Then, under the assumption that there exists no parameter uncertainty in $\mathbf{H}_f$, $\mathbf{K}_f$, and $\mathbf{N}_f$ of Eq. (13), the error dynamics becomes

$$\ddot{\mathbf{e}}_f + \mathbf{K}_{fv} \dot{\mathbf{e}}_f + \mathbf{K}_{fp} \mathbf{e}_f = \mathbf{0},$$

and the joint errors are asymptotically stable.

4.2 CG Motion Servo Controller

In order for the base link (the CG of the biped robot) to track reference base link motions, we need to consider the dynamic equations for the entire links including the free leg. Substituting $\ddot{\mathbf{q}}_f$ in Eq. (12) and $\ddot{\mathbf{q}}_s$ in Eq. (3) into Eq. (2), we can get

$$\tilde{\mathbf{R}} \mathbf{a}_0 + \mathbf{P}_s \mathbf{f}_s + \tilde{\mathbf{S}} = \mathbf{0} \tag{14}$$

where

$$\tilde{\mathbf{R}} = \mathbf{R} - \mathbf{Q}_s \mathbf{A}_s^{\#} \mathbf{B}_s - \mathbf{Q}_f \mathbf{H}_f^{-1} \mathbf{K}_f$$
$$\tilde{\mathbf{S}} = \mathbf{S} + \mathbf{Q}_f \mathbf{H}_f^{-1} \tau_f - \mathbf{Q}_s \mathbf{A}_s^{\#} \mathbf{C}_s - \mathbf{Q}_f \mathbf{H}_f^{-1} \mathbf{N}_f.$$

Matrix $\mathbf{A}^{\#}$ denotes the pseudo-inverse matrix of matrix $\mathbf{A}$. By combining Eq. (3) and the dynamics of the supporting leg only in Eq. (1), we can obtain a relationship without the term $\ddot{\mathbf{q}}_s$, which then can be substituted into Eq. (14), resulting in the relation between the base link acceleration and the control torque for the supporting leg, which is expressed as

$$\tilde{\mathbf{K}}_s \mathbf{a}_0 + \tilde{\mathbf{N}}_s = \tau_s \tag{15}$$

where

$$\tilde{\mathbf{K}}_s = \mathbf{K}_s - \mathbf{H}_s \mathbf{A}_s^{\#} \mathbf{B}_s - \mathbf{D}_s \mathbf{P}_s^{-1} \tilde{\mathbf{R}}$$
$$\tilde{\mathbf{N}}_s = \mathbf{N}_s - \mathbf{H}_s \mathbf{A}_s^{\#} \mathbf{C}_s - \mathbf{D}_s \mathbf{P}_s^{-1} \tilde{\mathbf{S}}.$$

Using Eq. (15), the computed control torque for the supporting leg can be computed such that the base link tracks its reference motion. Similarly to the computed torque method for manipulators, the computed torque for the leg is

$$\tau_s = \tilde{\mathbf{K}}_s (\mathbf{a}_0^d - \mathbf{u}_s) + \tilde{\mathbf{N}}_s \tag{16}$$

where $\mathbf{a}_0^d$ is the reference acceleration of the base link, and $\mathbf{u}_s$ is the linear error feedback control signal. A PD controller is used in the paper similarly to the case of the free leg and thus

$$\mathbf{u}_s = -\mathbf{K}_{sv} \dot{\mathbf{e}}_s - \mathbf{K}_{sp} \mathbf{e}_s$$

where $\mathbf{e}_s$ is the *position error* vector of the base link, which can be computed using the measurement of the leg joint angles and the forward kinematics. Then, the error dynamics of the supporting leg becomes

$$\ddot{\mathbf{e}}_s + \mathbf{K}_{sv} \dot{\mathbf{e}}_s + \mathbf{K}_{sv} \mathbf{e}_s = \mathbf{0}, \tag{17}$$

and can be stabilized.

5 Simulations

Simulations of a 7-link biped robot are done in order to compare the performance of the proposed method and that of the inverted pendulum mode. The parameters of the biped robot used in the simulations are shown in Table 1. The parameters for generating the walking pattern are also shown in Table 2. In computing β, the free leg mass concentrated at its foot, m, is assumed to be 1, 2, and 3 kg, which are slightly less than or equal to actual 3 kg, and M to be 13 kg. The reference motions of the base link generated by the proposed linear GCIPM and the linear inverted pendulum mode are shown in Fig. 4, which indicates that the maximum acceleration of the proposed method is slightly higher than that of the inverted pendulum mode.

Table 1: Biped robot model parameters

	Mass (kg)	Length (m)
Base Link (Link 0)	10	0
Link 1 of Each Leg	1.0	0.3
Link 2 of Each Leg	1.0	0.3
Link 3 of Each Leg	1.0	0.1

Table 2: Walking pattern parameters

Parameters	Symbol	Dimension
Step Time	T	1 sec
CG Height	H_z	0.5 m
Stride	S	0.2 m
Maximum Foot Height	h_f	0.1 m

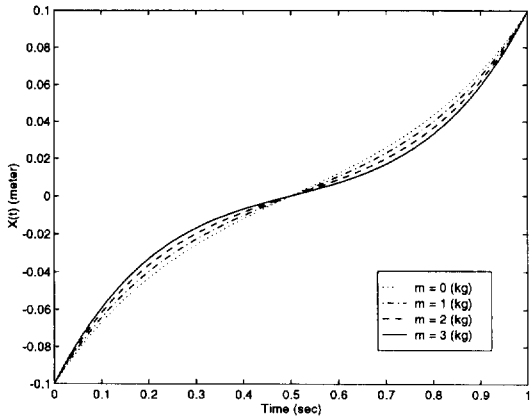

Figure 4: The reference motions of the base link with different magnitude of the base-link mass.

The actual ZMP movements for the left and the right legs, given the reference motion of the base link, are shown in Fig. 5. They indicate that motions of the ZMP are almost periodic except for the starting phase, and that the ZMP stays closer to zero when the proposed walking pattern is implemented.

From this, we can conclude that the proposed motion is more stable even without a separate active ZMP controller. Figure 6 displays graphic simulation snapshots of the walking biped robot.

6 Conclusions

In this paper, we constructed a biped robot simulator and proposed the GCIPM to generate walking patterns, which is *easily* applied to any types of biped robots, and servo controllers based upon the computed torque control method. And its tracking performance is verified through simulation.

Simulations are performed for a 7-link biped robot. Simulation results show that the walking pattern generated by the proposed GCIPM is superior in terms of the stability to that by the inverted pendulum mode. They also show that the computed torque controllers work very well.

References

[1] A. Takanish, M. Tochizawa, H. Karaki, and I. Kato, "Dynamic biped walking stabilized with optimal trun and waist motion," *Proceedings of the IEEE/RSJ International Workshop on Intelligent Robotics and Systems*, pp. 187–192, 1989.

[2] J. Yamaguchi, A. Takanish, and I. Kato, "Development of a biped walking robot compensating for three-axis moment by trunk motion," *Proceedings of the IEEE/RSJ International Workshop on Intelligent Robotics and Systems*, pp. 561–566, 1993.

[3] S. Kajita and K. Tani, "Study of dynamic biped locomotion on rugged terrain: Derivation and application of the linear inverted pendulum mode," *Proceedings of the IEEE International Conference on Robotics and Automation*, pp. 1405–1411, 1991.

[4] S. Kajita and K. Tani, "Experimental study of biped dynamic walking in the linear inverted pendulum mode," *Proceedings of the IEEE International Conference on Robotics and Automation*, pp. 2885–2891, 1995.

[5] Y. Fujimoto and A. Kawamura, "Three dimensional digital simulation and autonomous walking control for eight-axis biped robot," *Proceedings of the IEEE International Conference on Robotics and Automation*, pp. 2877–2884, 1995.

[6] S. Y. Oh and D. E. Orin, "Dynamic computer simulation of multiple closed-chain robotic mechanisms," *Proceedings of the IEEE International Conference on Robotics and Automation*, pp. 15–20, 1986.

[7] M. W. Walker and D. E. Orin, "Efficient dynamic computer simulation of robotics mechanism," *Journal of Dynamic Systems, Measurement, and Control*, vol. 104, pp. 205–211, 1982.

[8] J. J. Craig, *Introduction to Robotics: Mechanics and Control*. Addison-Wesley, 1986.

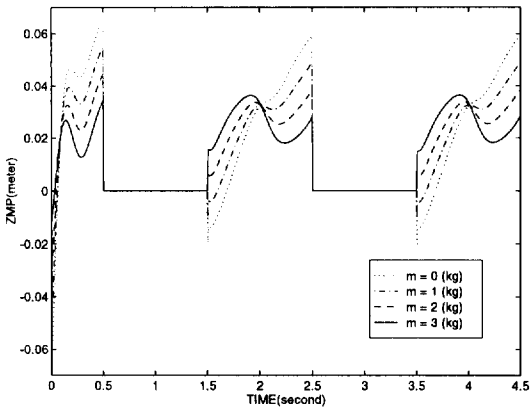

(a)

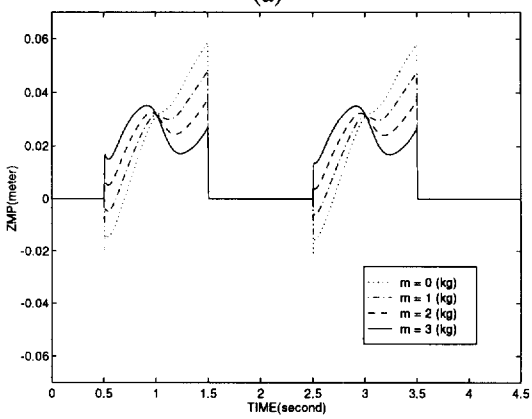

(b)

Figure 5: The ZMP stays closer to 0 for (a) the right foot and (b) the left foot when the GCIPM ($m \neq 0$) is used than when the linear inverted pendulum mode ($m = 0$) is used.

[9] F. L. Lewis, C. T. Abdallah, and D. M. Dawson, *Control of Robot Manipulators*. Macmillan, 1993.

[10] L. Sciavicco and B. Siciliano, *Modeling and Control of Robot Manipulators*. McGraw-Hill, 1996.

[11] M. Vukobratovic, B. Borovac, D. Surla, and D. Stokic, *Biped Locomotion: Dynamics, Stability, Control and Application*. Springer-Verlag, 1990.

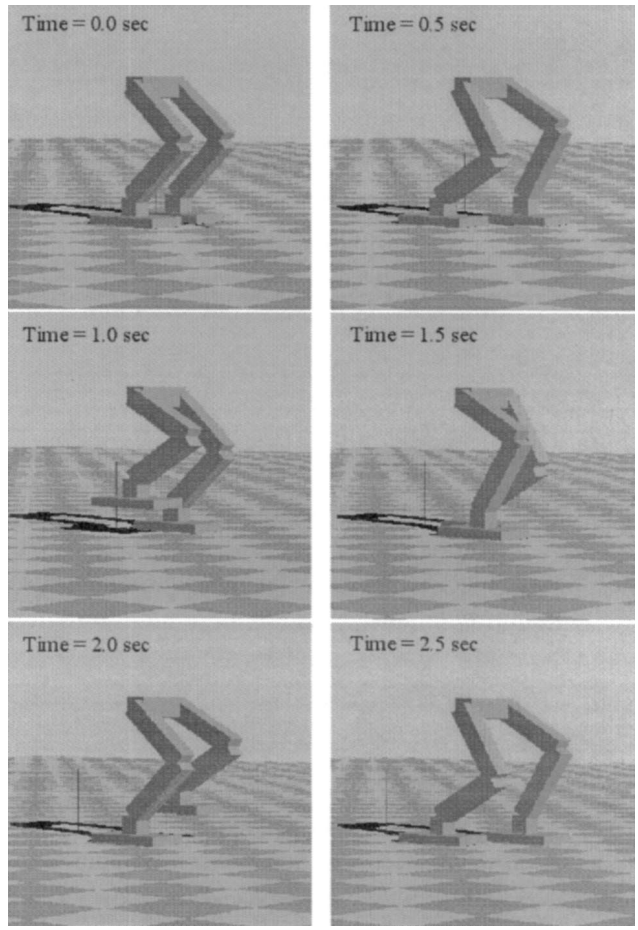

Figure 6: Walking of the biped robot in a simulation.